Fabricating colloidal particles with photolithography and their interactions at an air-water interface

A. B. D. Brown,[1,*] C. G. Smith,[1,†] and A. R. Rennie[2,‡]
[1]*Semiconductor Physics, Cavendish Laboratory, Madingley Road, Cambridge CB3 0HE, United Kingdom*
[2]*Department of Chemistry, Kings College London, Strand, London WC2R 2LS, United Kingdom*
(Received 15 February 2000)

A technique for fabricating nonspherical colloidal particles using photolithography has been developed. The particles are plate shaped and their profile within the plane of the plate is defined by a lithography mask and so can be any form desired. The thickness of the particles can also be controlled by varying the amount of material in the particle, and also by using the stresses induced during the evaporation of materials to distort the particles out of the plane. The particle-particle interactions can be tailored and made anisotropic by coating different faces of the particles with different chemicals or by making them of different materials. This technique is used to produce curved disks that are hydrophobic on their convex face and hydrophilic on their concave face. These particles are studied at an air-water interface, where the majority lie with their hydrophobic face uppermost. The curvature of the particles distorts the water surface in a manner that can be described by a series expansion. The symmetry of this function is used to explain the interactions of the particles and the resulting ordered flocculated structures observed. Such anisotropic forces in two dimensions have not been studied previously on a colloidal length scale to our knowledge and extend the field of control of particles at interfaces.

PACS number(s): 68.10.Cr, 61.20.−p, 82.70.Dd, 68.45.Gd

I. INTRODUCTION

Ordered structures of colloidal particles can give rise to bulk phenomena that are very different from those displayed by disordered structures. A classic example of this is the colored patterns observed in opal. Order is known also to greatly affect the electrical and rheological properties of colloidal dispersions. In the absence of an external field, spheres have been observed to crystallize into a variety of crystalline structures [1,2]. More complex crystal structures have been formed by mixing different sizes of spheres, where smaller spheres pack into the interstices between the larger spheres [3].

Despite the range of structures that could be observed with nonspherical particles, very few reports [4–7] have been made of ordered phases in such dispersions. This is primarily due to the difficulties associated with preparing dispersions of nonspherical particles that are uniform enough to allow crystallization. In this paper we present a method of preparing dispersions of nonspherical particles using photolithographic techniques. This method not only allows particles to be prepared in a very monodisperse manner but also allows platelike particles of any shape within the plane of the plate to be prepared. We also investigate bending the particles as a method of controlling their shape in the third dimension. Photolithography also has the potential to allow the introduction of chemical anisotropy in addition to anisotropy in the shape of the particles.

Crystallization of colloidal particles has often been studied in two dimensions, for example, at a fluid-fluid interface. This is experimentally convenient as it allows the dispersion to be observed using the third dimension. It also introduces capillary interactions between the particles, which are not present in three dimensions in the absence of a fluid-fluid interface. These capillary interactions arise from the way that the particles distort the fluid-fluid interface. Distortions caused by the weight of the colloidal particles give rise to attractive interactions as described by Chan, Henry, and White [8]. Using nonspherical particles, it is possible to create more complex distortions. These distortions can then be adjusted to create and control directional capillary forces between particles. Bowden *et al.* [9] demonstrated the effect of such directional forces with particles several millimeters across. In contrast, this paper describes methods that allow control of the capillary force on a colloidal length, so allowing structures to be formed on the length scale of a few micrometers. The technique developed here would also be applicable to particles on the length scale of a few hundred nanometers.

II. MAKING COLLOIDAL PARTICLES WITH CONTROLLED SHAPE

Photolithography can be used to define a two dimensional pattern in a layer of photoresist. A substrate is coated with a thin layer of photoresist (typically 0.5–5 μm) by spin coating. The pattern is transferred from a mask onto the photoresist by exposing the layer of photoresist to UV radiation through the mask. The photoresist is then developed. A positive photoresist (Shipley S1813) was used in this work, where the area exposed through the mask is then removed by the developer. The mask is usually created with a resolution

*FAX: +44 1223 337271. Electronic address: abdb1@cus.cam.ac.uk
†FAX: +44 1223 337271. Electronic address: cgs4@cam.ac.uk
‡FAX: +44 207 8482810. Electronic address: rennie@colloids.ch.kcl.ac.uk

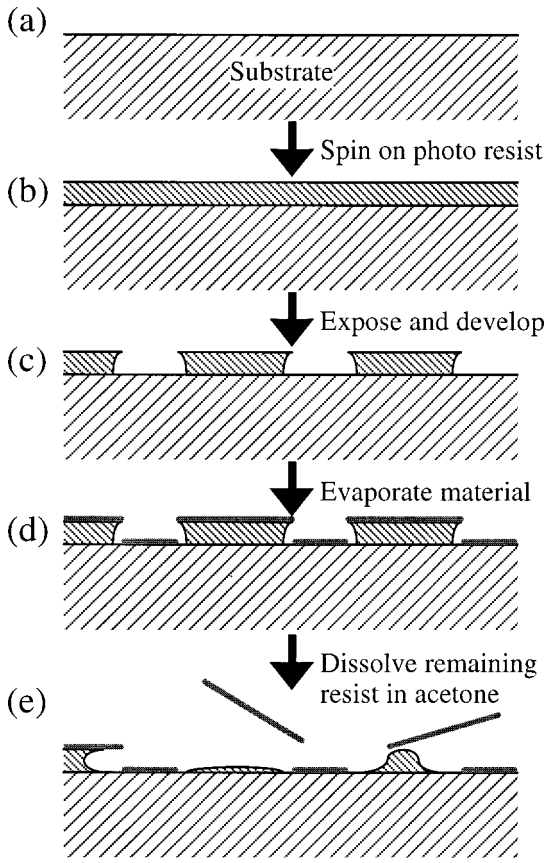

FIG. 1. Particles can be fabricated by evaporation using the following process. (a) A clean substrate is taken. (b) It is spin coated with photoresist. (c) It is exposed, soaked in chlorobenzene to harden the surface, and developed. (d) Materials are evaporated onto the substrate. (e) The substrate is placed in acetone, where the photoresist dissolves, releasing the particles.

of a fraction of a micrometer using electron beam lithography. The resolution permitted by photolithography using commercial apparatus is around 0.3 μm. With the equipment available for this work a resolution down to a micron was possible. This resolution limit meant that particles were typically made a number of microns across, with features a few microns in diameter. Particles of this size are then ideally suited for investigation using optical microscopy. In order to keep Brownian motion of the particles significant, the particles were made very thin, typically between 40 and 200 nm.

A. Evaporated particles

A plain, flat substrate [see Fig. 1(a)] was chosen which provides good adhesion with the first evaporated material. Typically either a glass slide or a gold coated glass slide was used. A layer of photoresist was spun onto the upper surface, giving a layer 1.3 μm thick [see Fig. 1(b)]. The photoresist was exposed to ultraviolet light through a mask so that each area to become a particle was not exposed. The substrate was then placed in chlorobenzene for a few minutes to harden the top surface of the photoresist. After development this gave a profile with a slight undercut as shown schematically in Fig. 1(c). The desired material(s) of the particles was (were) evaporated onto the surface [see Fig. 1(d)]. The substrate was then placed in acetone to dissolve the remaining photoresist, allowing the particles to lift off into the acetone [see Fig. 1(e)]. The particles were resuspended after centrifugation twice in acetone, then in ethanol, and finally in water.

The cleanliness of the resulting dispersion in terms of particulate contaminants depends crucially on what (besides the desired particles) lifts off into the acetone. Large areas of photoresist around the patterned area will be coated in evaporated material, which can come off and break up to form contaminants. To avoid this problem there must be no regions of photoresist that are not particles after developing. Using a mask that is clear except for the particles and then exposing the whole substrate can achieve this. Alternatively, it was observed that areas of material on photoresist a few millimeters across lift off into acetone much quicker than the particles, which are only a few micrometers across. This difference can be exploited to remove large areas of evaporated material on a continuous layer of photoresist into acetone, which is then discarded before transferring the substrate into clean acetone, where the particles are allowed to come off the substrate. A further consideration is that the evaporated material must adhere well to the substrate or else regions of evaporated material between the particles may come off the substrate in the acetone. For this reason a substrate material must be chosen that has good adhesion with the first evaporated layer.

B. Nonevaporated particles

Silicon dioxide particles were prepared from silicon wafers with a 200 nm oxide layer [see Fig. 2(a)]. A layer of photoresist was spun onto the upper surface, giving a layer 1.3 μm thick [see Fig. 2(b)]. The photoresist was then exposed to ultraviolet light through a mask so that each area to become a particle was not exposed. After development this gave a profile as shown schematically in Fig. 2(c). The wafer was placed in buffered hydrofluoric acid, to etch through the exposed area of silicon dioxide [see Fig. 2(d)]. The wafer was then placed in a solution composed of 23.4% KOH, 13.3% isopropanol, and 63.3% H_2O by weight at 80 °C. This etches the silicon away from under the particles, allowing them to lift off into the KOH [see Fig. 2(e)]. However, this solution also very slowly etches silicon dioxide. Consequently, once the particles lifted off the wafer, the etching was quenched by cooling the dispersion to room temperature, and the particles were immediately centrifuged out of the dispersion and repeatedly resuspended in water until the *p*H of the dispersion was found to be neutral.

This method of particle preparation allows particles to be made out of materials that cannot easily be evaporated. This technique could be adapted to make colloidal particles out of silicon or other semiconductors, allowing the particles to consist of semiconductor devices [10].

C. Cleaning particles

In order to remove all traces of photoresist and other organic material, the particles were cleaned in a H_2O_2:H_2SO_4:H_2O (1:1:5) solution, and then repeatedly washed in pure water. In order to measure the contact angle of the resulting surfaces, a number of large planar surfaces were prepared and cleaned in the same manner. A drop of

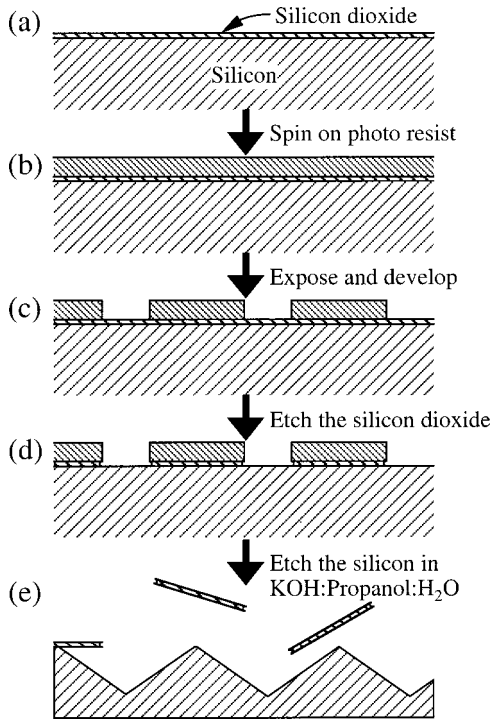

FIG. 2. Silicon dioxide particles can be fabricated by etching an oxidized silicon wafer using the following process. (a) A clean, oxidized silicon wafer is taken. (b) It is spin coated with photoresist. (c) It is exposed and developed. (d) The exposed oxide layer is etched away with buffered hydrofluoric acid. (e) The silicon is etched with a hot KOH solution saturated with propanol, releasing the particles.

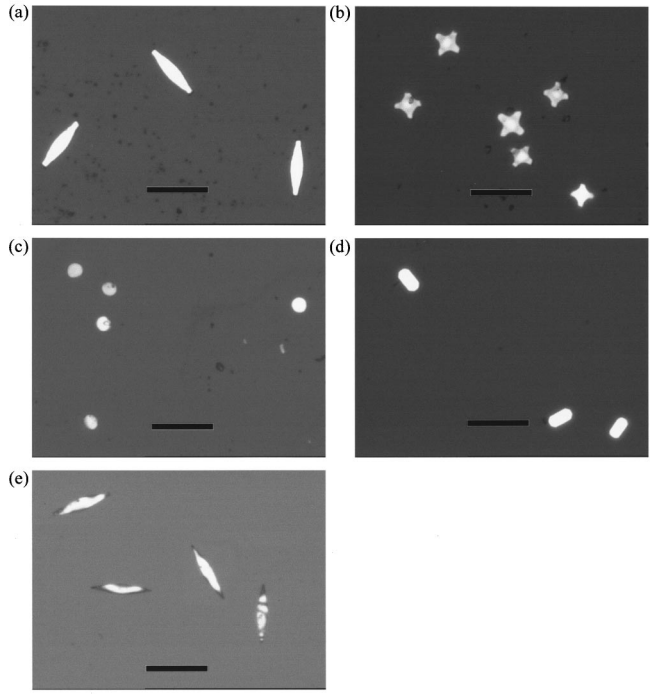

FIG. 3. Particles fabricated using the evaporation technique: (a) gold diamonds (200 nm), (b) Nichrome and gold crosses (20 and 20 nm, respectively), (c) Nichrome and gold disks (10 and 40 nm, respectively), and (d) gold rectangles (100 nm). (e) Silicon dioxide diamonds (200 nm) fabricated using the etching technique. The scale bar in all the figures is 20 μm long.

water was then placed on the surface and the contact angle measured. It was found that after cleaning in this manner a Nichrome (80:20 nickel:chromium alloy) surface was very hydrophilic (contact angle with water was less than 5°). In contrast, gold surfaces remained quite hydrophobic with a contact angle of around 90°.

Due to the two dimensional nature of this fabrication technique, the number of particles made is small by colloidal standards. The evaporators used were designed to expose only 30 cm^2 of patterned substrate, yielding of the order of 10^7 particles.

D. Chemical patterning

As well as making particles anisotropic in shape, particles can also be made anisotropic in terms of their interactions. One way to achieve this is to make the surface of the particles chemically anisotropic so that the charge, hydrophobic/philic nature, or steric coat on the surface is not uniform over the particle surface.

The simplest case is where the particles are made by evaporating two different materials so that the particles have one material on one face and another material on the opposite face. More complex patterning of the surface could be envisaged, by evaporating a thin second material at an angle so that some of the edges of the particle are coated with the second material while others are not. An alternative technique would be to pattern directly onto the top surface of the particles using an aligned second mask.

Well characterized surface chemistry such as thiol and chlorosilane reactions [11,12] can be used to graft a monolayer of an organic molecule onto the surface of a particular material. If a particle is made with a number of different materials, then different organic molecules can be grafted onto the different materials exposed. This would allow the surface chemistry of two surfaces of one particle to be controlled independently [13].

E. Particles made

Figures 3(a)–3(d) show a range of particle shapes that have been made using the evaporation technique described above. The crosses in Fig. 3(b) were made from a mask of a cross, 10 μm from end to end and with arms 2 μm wide. The crosses had slightly different dimensions across the mask, giving rise to a small range of particle sizes as clearly illustrated in Fig. 3(b). The resolution of the process has broadened the arms and rounded the corners. However, as mentioned earlier, this is simply a limitation of the apparatus used in this work, rather than of the technique. The diamonds [see Fig. 3(a)] and the rectangles [see Fig. 3(d)] have slightly bulbous ends. This is caused by optical effects due to a gap between the mask and the photoresist layer during exposure. Again, commercial apparatus is able to overcome this technical difficulty.

Figure 3(e) shows some silicon dioxide particles made using the etching technique described above. The varying intensity across the particle arises from interference between the particle surfaces and the glass slide the particle is resting on.

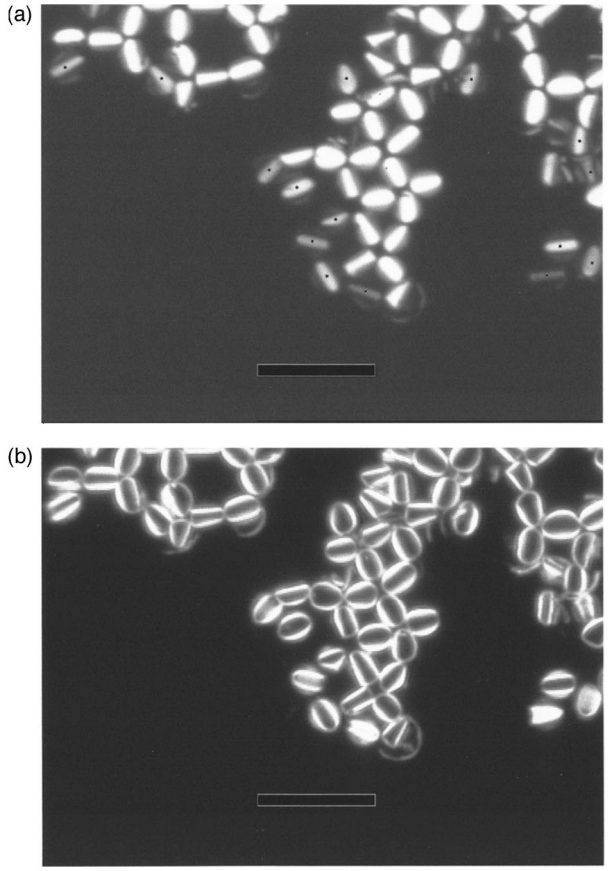

FIG. 4. Curved particles made by evaporation of Nichrome and gold (50 and 20 nm, respectively) on the surface of water. (a) Bright field showing reflection from the central, horizontal region. Particles with Nichrome surface uppermost are marked with a spot. (b) Dark field showing reflection from surfaces tilted at an angle between 22° and 26° to the horizontal. The scale bar is 20 μm long.

By evaporating 50 nm of Nichrome and then 20 nm of gold, curved particles were synthesized as shown in Fig. 4(a). The diameter of the disks is around 5 μm. The optical microscope shows a bright line across the particle. This region of the particle reflects the incident cone of light back into the microscope. The rest of the particle is at too great an angle to do this. In dark field the incident light is in the form of a hollow cone. In this arrangement [see Fig. 4(b)] two bright lines can be seen from each particle, where the surface of the particle is at the correct orientation to reflect the incident light into the lens. The radius of curvature can be estimated from the thickness of the line of reflected light in bright field and the distance between the lines of reflected light observed in dark field. These measurements give a radius of curvature of 4–5 μm. The particles appear elliptical in Figs. 4(a) and 4(b). This is due to the fact that the very edges of the particles are too tilted to reflect light into the microscope. Disks with a radius of curvature of 4 μm are only 6% narrower than they are long in plan view.

The curvature is a result of the stress induced during the evaporation of the metals, and consists of an intrinsic component that depends upon impurities and incomplete ordering during the evaporation, and a thermal component that depends on the different thermal-expansion coefficients of the two materials and the temperature of deposition and inspection [14]. It was found that the radius of curvature could be most conveniently controlled by varying the thickness of gold and Nichrome.

III. ANISOTROPIC FORCES AT THE AIR-WATER INTERFACE

In general there are three types of significant force present between charged particles trapped at an air-water interface. These are van der Waal's attraction, electrostatic repulsion, and a capillary interaction. With isotropic, spherical particles the capillary interaction is always attractive and arises from the deformation of the water surface due to the weight of the colloidal particle. This deformation provides a gravitational well that other particles can fall down. The nature of this attractive force is described in some detail by Chan, Henry, and White [8].

Of these forces, the van der Waal's attraction decays the most quickly with distance, while the capillary attraction decays most slowly. Typically, however, on a colloidal length scale the capillary attractive force is small in comparison to k_BT, due to the small weight of the particles, and so can be ignored.

Anisotropic particles introduce a new form of the capillary energy that can arise from distortions in the surface of the water induced by the chemical or physical anisotropy of the particles. In order to estimate the strength and range of the resulting interactions it is necessary to consider the nature of the induced distortion.

A. Distortion caused by a single particle

If an infinite line of the air-water interface is raised above or lowered below the equilibrium height, then the distortion decays exponentially in a direction perpendicular to the line on a length scale of λ^{-1} where λ is given by

$$\lambda = (\rho g/\gamma)^{1/2}$$

ρ is the difference in density between water and air, g is the acceleration of gravity, and γ is the surface tension or energy of the air-water interface.

For an air-water interface, λ^{-1} is approximately 2.7 mm. We are concerned with interactions between particles on the length scale of a few microns; therefore $r\lambda \ll 1$ where r is the distance from the center of the particle. In this limit the distortion around a small circle of the interface that is raised or lowered is given by $-A\ln(r\lambda)$, where A is a constant governing the magnitude of the distortion and r is the radial distance from the center of the distortion [8]. Clearly this equation implies the condition that $r \neq 0$, which is as expected since a finite force cannot be applied to an infinitely small air-water interface.

At large distances compared to the size of the particle, the distortion of the air-water interface due to that particle can be described by the sum of monopole, dipole, quadrupole, and higher order terms. In order to produce a distortion with a monopole component, a force needs to be applied to the particle perpendicular to the air-water interface. An example of such a force is that provided by gravity; however, with colloidal sized particles the monopole distortion caused by gravity is usually small and so can be neglected. In a similar

way, in order to produce a distortion with a dipole component, a torque needs to be applied to a particle about an axis in the plane of the air-water interface. In contrast to the monopole and dipole distortions, distortions comprising just quadrupole and higher order terms do not require an external force or torque to be applied to the particle. This is due to the fact that for quadrupole and higher order terms, the forces and the resulting torques applied to the particle by the air-water interface balance across the particle. Thus a quadrupole, where in general two points are distorted one way and two distorted the other, is the simplest equilibrium distortion that a particle could induce in the absence of an external field. If for distortions of small magnitude the magnitude of the distortion at any point is taken to be additive, then in cylindrical coordinates (r,θ,z) the resulting displacement of the interface from equilibrium around a quadrupole is given by the form

$$z(r,\theta)=B\cos(2\theta)/r^2, \tag{1}$$

where B is a constant.

One way to introduce such distortions is to place a particle on the water surface which has some edges that are hydrophilic, while other edges are hydrophobic. The hydrophilic edges would attract the water and so distort the water surface upward, while the hydrophobic edges would distort the water surface downward. These distortions should result in an attraction between like sides, and a repulsion between unlike sides. Particles of this nature have been made on a centimeter length scale by Bowden *et al.* [9]. However, with macroscopic particles the weight or buoyancy of the particles also significantly distorts the surface of the water, so that areas of the particles that pull the surface down are more strongly attracted to each other than areas that pull the surface up.

In this paper surface distortions are introduced by placing curved particles on the surface of the water that have hydrophilic lower faces and hydrophobic upper faces. Such particles can be made three orders of magnitude smaller than those used by Bowden *et al.*, so that the potential energy from the capillary interaction due to the weight or buoyancy of the particles is less than k_BT.

Consider a thin disk shaped particle that is bent out of the plane of the disk by laying it on the surface of a cylinder as shown in Fig. 5. In the case that the radius of the cylinder is much greater than the radius of the disk, the edge of the particle can be approximated by the following equation in cylindrical coordinates:

$$z=z_0\cos(2\theta), \tag{2a}$$

$$r=r_0, \tag{2b}$$

where r_0 is the radius of the disk and z_0 is the maximum distortion of the disk.

The energy associated with the distortion of the air-water interface due to such a particle at the interface can be divided into the energy associated with the increase in surface area of the water, E_{SA}, and that associated with the gravitational potential energy of the displaced water, E_G. Consider a small area of the water surface with dimensions δr and $r\,\delta\theta$. Assuming that the gradient of the water surface is small so

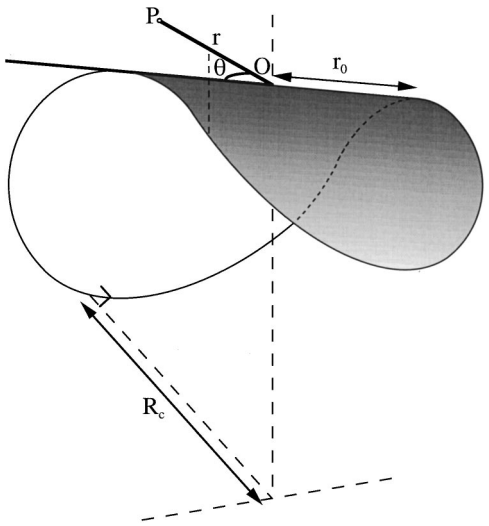

FIG. 5. A disk curved by laying it on the surface of a cylinder. The top convex surface is hydrophobic, while the bottom concave surface is hydrophilic. The radius of curvature of the disk is R_c and the radius of the disk is r_0. For the disk shown, R_c and r_0 are similar in magnitude. A point P in a two dimensional plane tangential to the particle surface and containing the undistorted diameter of the disk is defined by θ, the angle between the vector $\overline{OP}$ and the undistorted diameter of the disk, and the radial distance r, the magnitude of the vector $\overline{OP}$.

that fourth order terms in $\delta z/\delta r$ and $\delta z/(r\,\delta\theta)$ can be neglected, the increase in surface area can be approximated by

$$\tfrac{1}{2}(\delta z/\delta r)^2\,\delta r\,r\,\delta\theta+\tfrac{1}{2}r^2(\delta z/\delta\theta)^2\,\delta r\,r\,\delta\theta,$$

which is the sum of the increase in surface area due to the gradient in the radial direction and that due to the gradient in the tangential direction. Substituting expressions for dz/dr and $dz/d\theta$ derived from Eq. (1) gives

$$2(z_0r_0^2)^2(\cos^2 2\theta/r^5)\,\delta\theta\,\delta r+2(z_0r_0^2)^2(\sin^2 2\theta/r^5)\,\delta\theta\,\delta r.$$

The symmetry of the two halves of this equation shows that around a quadrupolar distortion, the surface energy is equipartitioned between the energy arising from the gradient in the radial direction and that arising from the gradient in the tangential direction. Thus the energy stored due to the increased surface area at any radius is independent of θ. Integrating over all of space gives

$$E_{\mathrm{SA}}=\pi z_0^2\gamma.$$

The gravitational potential energy can be similarly calculated and is given by

$$E_G=g\rho z_0^2r_0^2\pi/4.$$

For a disk of radius $r_0=2.5\,\mu$m and laid on a cylinder of radius R_c, giving a maximum distortion $z_0=0.31\,\mu$m, the resulting energy of the distorted air-water interface is

$$E_{\mathrm{SA}}=2.2\times10^{-14}\ \text{J};\ 140\ \text{keV};\ (5.4\times10^6)k_BT,$$

$$E_G=4.9\times10^{-21}\ \text{J};\ 31\ \text{meV};\ 1.2k_BT.$$

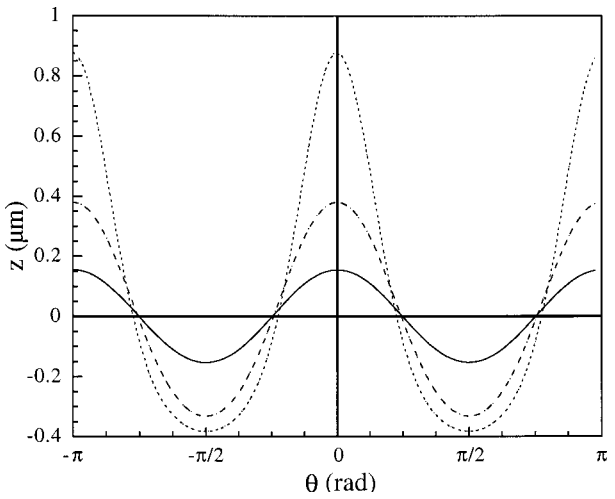

FIG. 6. The displacement of the air-water interface at a distance of 2.5 μm from the center of a disk with radius r_0 2.5 μm and a radius of curvature R_c 10 μm (solid line), 4 μm (dashed line), and 1.59 μm (dotted line).

While $\gamma \gg g\rho r_0^2/4$, i.e., for $r_0 \ll 5$ mm at the air-water interface, the energy associated with a quadrupolar distortion is primarily stored in the surface energy, and the gravitational potential energy can be ignored. For the particle dimensions described above the total energy of the distortion around a particle is five orders of magnitude larger than the thermal energy of a particle. This balance would be quite different if the radius of the particles were decreased by a factor of 10, while the radius of curvature was increased by a factor of 10. z_0 is approximately proportional to r_0^2/R_c, and so this would decrease the energy of the distortion by six orders of magnitude, making it comparable to the thermal energy of the particles.

It has been shown that a quadrupolar distortion has a uniform distribution of surface energy around it. Anisotropic components arise from terms of higher order than a quadrupole. These higher order terms were removed when the height of the edge of a particle was approximated to a sinusoidal function as given in Eq. (2). By numerically fitting a series of quadrupoles, octopoles, and higher order terms to an exact expression for the height of the edge of a curved disk, a more accurate expression for the profile of the water surface can be found. The following expression is the result of such a fit up to terms in $\cos(8\theta)/r^8$ for a disk of radius $r_0 = 2.5\,\mu$m and radius of curvature $R_c = 4\,\mu$m:

$$z = 2.252\cos(2\theta)/r^2 + 0.765\cos(4\theta)/r^4 + 0.995\cos(6\theta)/r^6 + 1.375\cos(8\theta)/r^8 \quad \mu\text{m}$$

if r is inserted in micrometers. This equation is clearly not valid for values of r less than the extent of the particle, and at $r = 2.5\,\mu$m the coefficient of the last term is a fraction of a percent of that of the total, thus suggesting that in this case these four terms give the value of z to an accuracy of better than 1%.

Figure 6 shows this function and two other values of R_c as a function of θ at $r = 2.5\,\mu$m. As the value of R_c is decreased, thus increasing the curvature, the displacement of the water surface is increased, as is the deviation of that displacement from the sinusoidal function of a purely quadrupolar distortion. As discussed earlier, the energy distribution around a quadrupolar distortion is uniform with angle. Variation in the surface energy distribution around a particle must therefore arise from the deviation of the distortion from a sinusoidal function. Along the axis of the curvature of the disk ($\theta = 0$) the distortion is sharper and higher than that of a sinusoidal function. Therefore around this direction the gradient and hence the energy stored in both the radial and tangential directions must be greater than that found in a sinusoidal distortion. In the perpendicular direction the distortion becomes correspondingly shallower and broader. Therefore around this direction the gradient and hence the energy stored in both the radial and tangential directions must be less than that found in a sinusoidal distortion. This means that the energy density stored in the surface of the water is greatest around the axis of curvature of the particle.

B. Interaction of distortions from different particles

A detailed calculation of the surface profile and hence the surface energy due to more than one particle would not be simple due to the multibody nature of the problem and the constraint that the particles are not distorted. However, the energy of the distortion around a single particle is much greater than k_BT, and so the energy of interaction between two particles is also likely to be large compared to k_BT. This assumption allows some useful observations to be made.

Consider the curved, disk shaped particles discussed above. Two of these particles must interact in such a way as to minimize the area of the air-water interface, and so minimize the energy of the system. If they come into contact oriented so that the points in contact are at the same height, then the energy of the distorted air-water interface due to the curvature of the particle around the point of contact and those nearly in contact is effectively canceled by the presence of the other particle. However, if one of these particles is rotated slightly so that the heights of the two points in contact are slightly different, then an almost vertical water surface must exist between the two particles. Such a surface would be very energetically unfavorable; for example, an area of 0.01 μm^2 has a corresponding energy of 7×10^{-16} J. This means that any packing of particles must be one in which the particles come into contact only where they distort the water surface by the same amount. Assuming the particles are not tipped by their interactions with other particles, this rule can be expressed by $\alpha = \beta$, where α and β are the angles between the line joining two particle centers and the orientation of each particle, as shown in Fig. 7.

If the energy of the particle interactions were small so that the particle-particle bonds could be broken, allowing particles to rearrange, then they would find an equilibrium configuration. If an external pressure were applied, this configuration would be expected to be the most dense packing permitted within the constraints that $\alpha = \beta$. A number of two dimensional structures are possible. Figure 8 shows some examples. The simplest is the square lattice shown in Fig. 8(a). In this configuration, however, the water surface in the interstices is very distorted, and almost ranges from fully raised to fully lowered. An arrangement with less distortion is the tilted square lattice shown in Fig. 8(b) where the par-

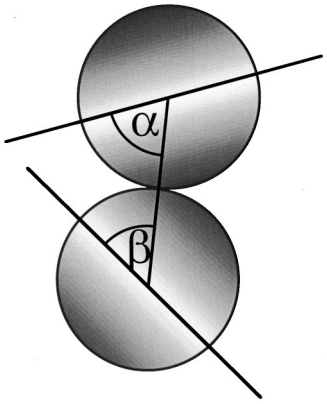

FIG. 7. If two particles are in contact then the vertical displacement near the point of contact would be expected to be the same; therefore α should equal β for all pairs of disks in contact on the water surface.

ticles have all been rotated by 45°. This is the most densely packed structure permitted by the constraint that $\alpha=\beta$. It is not possible to have a hexagonal close packed structure that fulfils this criterion; however, related structures can be imagined such as that depicted in Fig. 8(c).

If the binding energies are large compared with k_BT, so that the particles can rotate around each other, but not come apart once attached, the resulting structure will be governed by the dynamics of the way in which single particles are attracted to and bind to each other and clusters. If the distortion from each particle is taken to be additive then the resulting displacement of the water surface can easily be calculated and is shown in Fig. 9 for two configurations of three particles. Two particles would be expected to favor binding along their axis of curvature as the energy of the distorted air-water interface is greatest in this direction, due to the fact that the displacement of the surface and the rate of change of the displacement are both greatest in and around this direction, as illustrated in Fig. 6. Particles A and B are bound in such a manner in Fig. 9. The gradient and displacement of the water surface at a constant radius from the center of mass of such a bound pair are again a maximum at and around the ends of the structure. Thus if a particle C approaches, it will be more strongly attracted to the ends of the structure as shown in Fig. 9(b) than it will to the sides of the structure as illustrated in Fig. 9(a). An alternative argument is that if particle C approaches from the side as illustrated in Fig. 9(a) then there is an attractive force between it and particle A, while there is a repulsive force between the side of it and particle B. This repulsion will tend to push particle C around particle A, until it approaches from the end as shown in Fig. 9(b). These arguments suggest that particles will aggregate to form chains. At later stages and higher concentrations these chains might then aggregate together, as their sides would be weakly attractive. This would give rise to square packing as shown in Fig. 8(a), which would then distort to give the structure shown in Fig. 8(b). The structure shown in Fig. 8(c) would not be expected, as in order to form this structure particles would have to be attracted to the region where A and B join. This is not the case, as Figs. 9(a) and 9(b) clearly illustrate that there is a depressed (dark) region of the surface above and below the bound pair, which would act as a barrier to a particle that was attracted to the raised region between the bound pair.

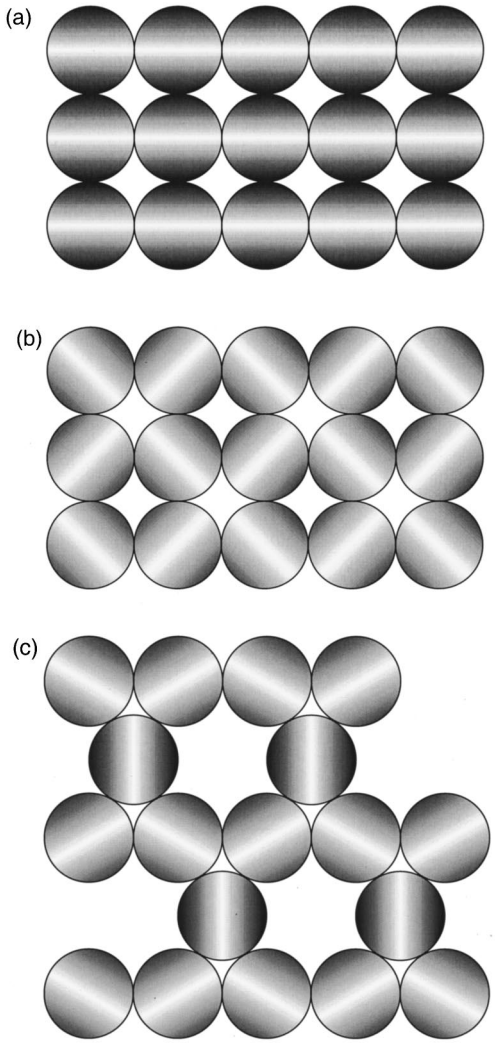

FIG. 8. Two dimensional packing structures on the water surface. The shading indicates the height of that area of the disk (the lightest areas are the highest). (a) A square packing formed from chains of disks joined side to side. The water in the interstices is very strained. (b) To relax the strain in the water in the interstices the particles could rotate by 45°, giving a tilted square lattice. (c) An alternative tessellating structure, based on hexagonal close packing with a vacancy to allow the rule that $\alpha=\beta$ to be followed for every pair in contact.

Once formed clusters would be quite rigid, and so would not distort when clusters come together. The final structure would thus consist of chains, and regions of tilted square lattice, clustered together in an open structure.

A third possibility is that the binding energies are such that particles, once in contact, cannot rotate around each other, as well as being unable to come apart. In this case chain formation might still be expected, as binding to the end of a bound pair would still be preferable to binding to the side, and so an approaching particle would tend to move toward the end of a bound pair. However, the resulting chains would not be nearly as uniform as in the previous case. These chains might attract each other and aggregate side by side, giving the square lattice shown in Fig. 8(a).

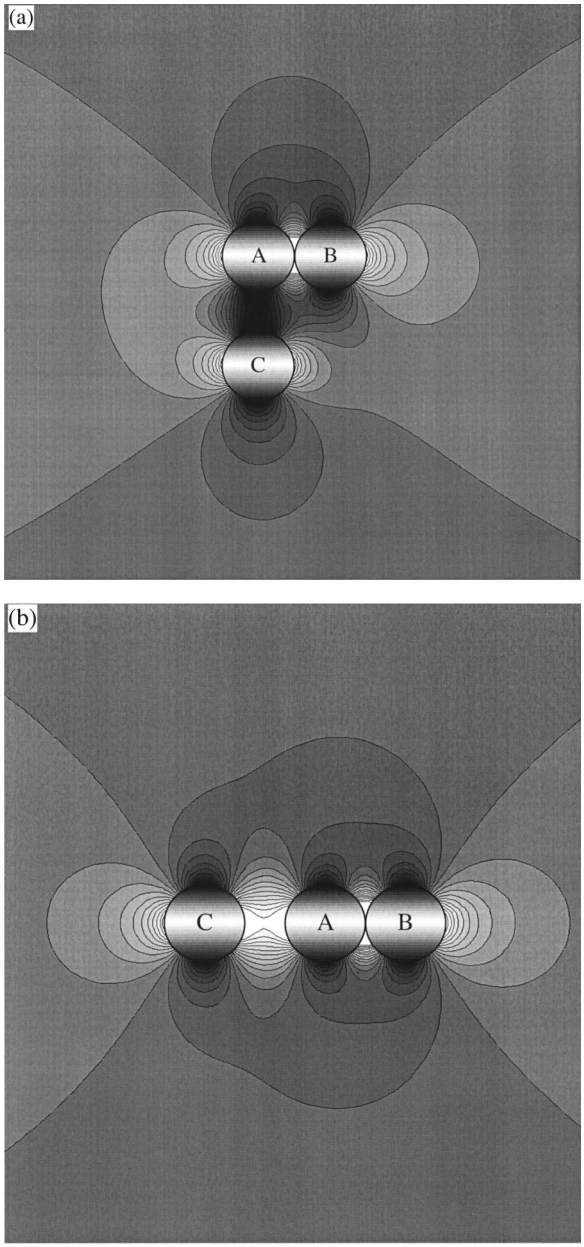

FIG. 9. Interactions of curved disks at the water surface; the shading indicates the height of the water surface (the lightest areas are the highest). (a) Two disks distort the water surface the least when they are in contact along the axis of curvature. Disk C is attracted to the side of disk A, but repelled by disk B. (b) Disk C is attracted to the end of a joined pair.

However, this structure would not be able to distort into the tilted square lattice shown in Fig. 8(b).

C. Experimental observations

The curved disks of Nichrome and gold shown in Fig. 4 have a radius of 2.5 μm and a radius of curvature of 4–5 μm. Therefore the height of the distortion that they will make on the surface of water will be approximately ± 0.38 μm ($z_0 = 0.76\,\mu$m). These disks were transferred to methanol by repeatedly centrifuging and resuspending the dispersion. A drop of the resulting dispersion was then placed on a clean water surface in a Langmuir trough mounted on a microscope. The particles aggregated to give small clusters, which then coalesced as the surface was compressed to give large clusters as shown in Fig. 10. Figure 4 is a magnification of the bottom of Fig. 10.

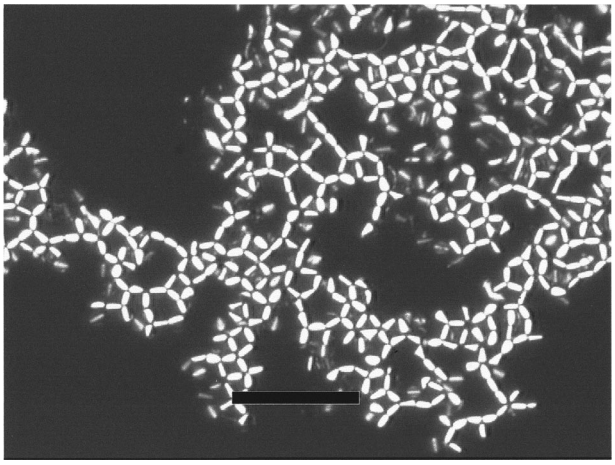

FIG. 10. A cluster of particles observed on the water surface. Figure 4 is a magnification of the lower left of this picture. The scale bar is 50 μm long.

Some particles appear only faintly in Figs. 4 and 10. These particles have their Nichrome surface upward, and account for 18% of the particles at the water surface, while the brighter particles (82%) have their gold surface upward. The particles with their Nichrome surface upward have been highlighted by spots in Fig. 4, as the difference in appearance between the Nichrome side and the gold side is much clearer when viewed in color when the gold appears yellow and the Nichrome gray. Which way up the particles lie can also be confirmed by viewing the particles in dark field. If half the incident cone of light is obscured then in general one of the two lines of reflected light disappears. From this the angle of the reflecting surface of the particle can be inferred, indicating which way the particle is curved.

The preference for the particles to lie with their gold surface uppermost is not surprising, as the gold surface of the particles is hydrophobic (contact angle of $\sim 90°$) while the Nichrome is hydrophilic (contact angle $<5°$). Particles placed on a glass substrate from a dispersion in methanol were observed lying both ways up in roughly equal numbers. The preference for particles to lie with their gold side upward when spread on the surface of the water could be due to the particles tumbling during the spreading process and the Nichrome side sticking to the water surface. Alternatively, the majority of the particles that lie with their gold surface down sink and are not observed.

Almost all the particles with their Nichrome surface uppermost showed interference fringes on the surface (not clear in the grey scale pictures shown in this paper), suggesting that the particles were covered by a thin film of water and inclined at an angle to the interface. The particles appeared to be prevented from sinking completely due to a few points pinned to the interface. Many of these partially submerged particles were also observed to remain unflocculated, and when flocculated were primarily observed around the edges of particle clusters. This is consistent with the observation that they are partially submerged, as this would reduce the

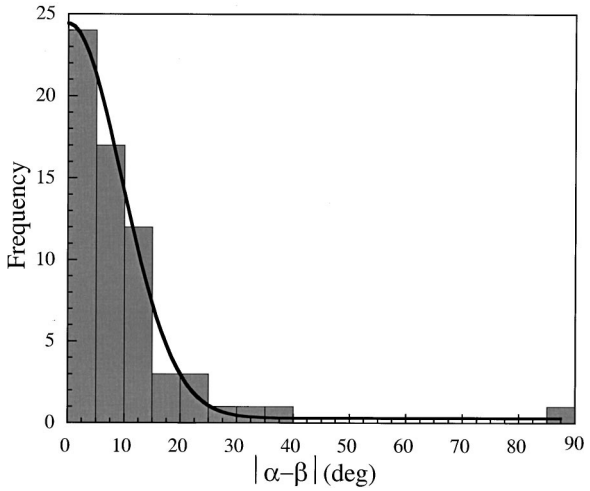

FIG. 11. A histogram of the magnitude of $\alpha-\beta$ over a cluster of 50 particles.

amount they distort the water surface and so reduce the attraction between them and other particles.

In the preceding section it was predicted that the particles would lie in such a way that the points of contact would have the same vertical displacement, or $\alpha=\beta$ as defined in Fig. 7. Figure 11 is a histogram of the magnitude of $(\alpha-\beta)$ taken from a clump of 50 particles. If the particles had no favored orientation then this histogram would show a uniform frequency at all angles. The strong peak at 0° with a half height at half width of 11° shows that there is a very strong preference for the particles to lie in the manner predicted.

Figure 10 shows regions where the particles form short chains, typically 3–5 particles long. Elsewhere in the sample much longer chains were observed, such as that shown in Fig. 12. The particles are connected along their axis of curvature. This is in agreement with the calculations in the previous section, which predicted that the small deviation from a quadrupolar distortion induced by a curved disk would mean that the equilibrium position for two particles to bond together would be in this orientation. It should be noted that the chain in Fig. 12 has no anomalous kinks, suggesting that the particles must be free to rotate around each other to reach the minimum energy configuration. The curvature of the chain is due to stress imposed by the barriers of the Langmuir trough compressing the structure.

A number of regions in Figs. 4 and 10 display ordered two dimensional structures. The primary pattern present is the tilted square lattice as illustrated in Fig. 8(b). The presence of this structure and the absence of any regions that show an untilted square structure [see Fig. 8(a)] also show that the particles must be free to rotate around each other.

On a larger scale, as shown in Fig. 10, the structure is quite open, confirming the calculation that the energy of interaction is sufficiently large to prohibit particle-particle bonds from being broken once formed.

The structures observed show a very strong correlation with the prediction that two particles in contact must be oriented so that $\alpha=\beta$. The structures agree closely with the calculations for particles with slightly distorted quadrupolar interactions, where the energy of the distortions is large compared to k_BT. In order to observe more highly ordered structures it would be necessary to investigate particles in a regime where the energy of particle-particle interactions is a few tens of k_BT. This could be achieved by investigating particles with a diameter in the region of 250 nm, and a radius of curvature over 10 μm. Such particles could be fabricated in a manner very similar to the evaporation technique described here, if electron beam lithography were used to pattern the photoresist instead of optical lithography.

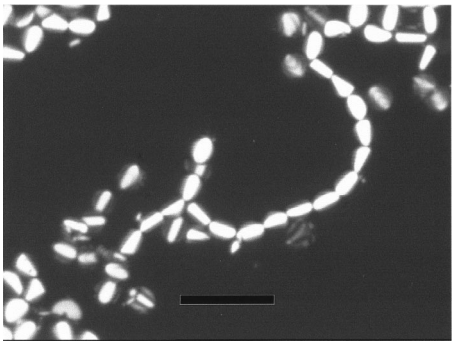

FIG. 12. A chain of particles observed. The scale bar is 20 μm long.

Attractive forces at interfaces between spheres have been reported [15] which cannot be explained in terms of simple electrostatic interactions. Uniform spheres can only cause a monopolar distortion of the water surface arising from the weight of the spheres. This is small for colloidal particles; however, if the surface of the spheres is not perfectly smooth on a length scale of a few tens of nanometers then the particle surface could distort the air-water interface in a similar manner, though on a smaller scale, to the particles discussed in this paper. Such distortion of the interface would provide weak, long range attractive forces. In a radial direction from the center of a sphere, the height of the water surface varies as $z=z_0r_0^nr^{-n}$, where z_0 is the magnitude of the distortion at the surface of the particle, and r_0 is the radial distance to the air-water-particle interfacial line. If the range of the force between two particles is taken to be the distance at which the magnitude of the distortion decays to a certain value, then if r_0 is doubled and z_0 remains unchanged the same value of z will be found at double the original value of r. Thus the range of this force would scale with the particle size if the length scale of the roughness of the particle surface remained constant. Such scaling of an attractive force would be consistent with the attraction observed by Ghezzi and Earnshaw [15].

IV. CONCLUSIONS

We have demonstrated a method of making colloidal particles using lithographic techniques. The techniques described allow plate shaped particles to be fabricated with any in-plane shape at a resolution permitted by the lithography used. A variety of shapes were fabricated, out of evaporated metals and etched silicon dioxide. This technique could easily be extended to allow fabrication of semiconductor particles, and could be performed with electron beam lithography to allow smaller particles with higher resolution features to be fabricated. It was found that particles could be shaped

in the third dimension by bending them with evaporation induced stress. This method was illustrated with disk shaped particles.

Disk shaped particles with one hydrophilic and one hydrophobic face, curved out of the plane of the disk, were studied at an air-water interface. These particles were found to distort the interface, giving rise to anisotropic forces between the particles. The distortion produced by one particle could be approximated by a quadrupole. However, in order to explain the formation of chains along the axis of the particles it was necessary to consider higher order terms. The resulting directional interactions between particles trapped at the interface caused ordered structures to form.

ACKNOWLEDGMENTS

A.B.D.B. thanks the Oppenheimer Trust and the Newton Trust for research funding.

[1] S. M. Clarke and A. R. Rennie, Langmuir **13**, 1964 (1997).
[2] Y. Monovoukas and A. P. Gast, J. Colloid Interface Sci. **128**, 533 (1989).
[3] S. M. Underwood, W. van Megen, and P. N. Pusey, Physica A **221**, 438 (1995).
[4] G. Oster, J. Gen. Physiol. **33**, 445 (1950).
[5] M. P. B. van Bruggen, F. M. van der Kooij, and H. N. W. Lekerkerker, J. Phys.: Condens. Matter **8**, 9451 (1996).
[6] A. B. D. Brown, C. Ferrero, T. Narayanan, and A. R. Rennie, Eur. Phys. J. B **11**, 481 (1999).
[7] F. M. van der Kooij and H. N. W. Lekkerkerker, J. Phys. Chem. B **102**, 7829 (1998).
[8] D. Y. C. Chan, J. D. Henry, Jr., and L. R. White, J. Colloid Interface Sci. **79**, 410 (1981).
[9] N. Bowden, A. Terfort, J. Carbeck, and G. M. Whitesides, Science **276**, 233 (1997).
[10] Cavendish Kinetics Ltd., International Patent No. PCT/GB97/02093 (1998).
[11] A. Ulman, *An Introduction to Ultra Thin Films* (Academic, San Diego, 1991).
[12] C. D. Bain and G. M. Whitesides, Science **240**, 62 (1988).
[13] B. R. Martin *et al.*, Adv. Mater. **11**, 1021 (1999).
[14] R. W. Hoffman, in *Physics of Thin Films*, edtied by G. Hass and R. E. Thun (Academic, London, 1966), Vol. 3, p. 211.
[15] F. Ghezzi and J. C. Earnshaw, J. Phys.: Condens. Matter **9**, L517 (1997).